PHYSICAL REVIEW B **78**, 081304(R) (2008)

Anomalous first-order Raman scattering in III-V quantum dots: Optical deformation potential interaction

Anabela G. Rolo,[1] Mikhail I. Vasilevskiy,[1,*] Mimoun Hamma,[2] and Carlos Trallero-Giner[3]
[1]*Centro de Física, Universidade do Minho, Campus de Gualtar, 4710-057 Braga, Portugal*
[2]*L.P.S., Faculté des Sciences Dhar Mehraz, BP 1796, Fés, Morocco*
[3]*Departamento de Física Teórica, Universidad de La Habana, Vedado, 10400 La Habana, Cuba*
(Received 2 June 2008; published 18 August 2008)

In contrast to the most commonly studied nanocrystals of II-VI materials, resonant Raman spectra of colloidal III-V quantum dots (QDs) show two almost equally intense peaks centered approximately at the longitudinal and transverse optical (TO) bulk phonon frequencies. The "anomalous" spectra of III-V QDs are explained in the framework of a microscopic theory for the first-order resonant Raman scattering, which takes into account the optical deformation potential (ODP) and Fröhlich exciton-phonon interactions—valid for spherical nanoparticles. It is obtained that: (i) the "anomalous" TO peak is mostly due to confined phonon modes with the angular momentum $l_p=3$; (ii) Raman intensity depends on the QD radius (R) as R^{-3} for the ODP mechanism, while for the Fröhlich one it is proportional to R^{-1}; and (iii) the relative intensity $I_{\mathrm{TO}}/I_{\mathrm{LO}}$ ratio value is higher in backscattering configuration for cross polarization than for parallel one. Raman spectra calculated within the Luttinger-Kohn Hamiltonian for the electronic states and a phenomenological theory of optical vibrations including rigorously both the mechanical and electrostatic matching boundary conditions explain the experimental data for InP QDs using bulk phonon parameters and ODP constant.

DOI: 10.1103/PhysRevB.78.081304 PACS number(s): 78.67.Hc, 63.20.K−, 63.22.−m

I. INTRODUCTION

In polar semiconductors there are two different mechanisms for electron-phonon coupling. Optical phonons produce a long-range electric field giving rise to the Fröhlich interaction. The momentum conservation in bulk crystals leads to the first-order Raman selection rule of dipole-forbidden longitudinal (LO) phonon scattering. The second independent electron-phonon [both LO and transverse optical (TO)] mechanism is via the dipole-allowed optical deformation potential (ODP). Choosing appropriate backscattering configurations, the electrostatic potential and mechanical deformation can be probed separately in the resonant Raman scattering (RRS) (see Ref. 1, and references therein). Due to the translational symmetry breaking in quantum dots (QDs), the stronger Fröhlich-type coupling becomes allowed in any geometry and it is generally assumed as the dominant effect.[2] Hence, typical RRS spectra observed for nearly spherical II-VI semiconductor nanocrystals (NCs) present a single asymmetric peak slightly below the bulk LO phonon frequency (ω_{LO}) while TO phonon is absent (see Ref. 3 for a recent review in QDs). However, a TO-type scattering was observed for III-V NCs such as InP and InAs.[4–7] Typical Raman spectra are shown in Fig. 1 for InP QDs with different mean diameter $\langle D\rangle$. It follows from the figure that the relative intensity of the TO-type peak with respect to the LO-type one ($I_{\mathrm{TO}}/I_{\mathrm{LO}}$) increases when the QD size decreases, which is consistent with previously reported studies.[4,5] We also found that $I_{\mathrm{TO}}/I_{\mathrm{LO}}$ is quite different for parallel ($\bar{Z}(X,X)Z$) and perpendicular ($\bar{Z}(X,Y)Z$) backscattering geometries. For instance, in the case of 3.8 nm QDs, it attains approximately one half for $\bar{Z}(X,X)Z$ and 80% for $\bar{Z}(X,Y)Z$. The peak positions are shifted with respect to the bulk TO and LO phonon frequencies, which becomes noticeable for the smaller size NCs. The transversal phonon peak is blueshifted while the LO one is redshifted. Finally, it is observed that both bands are asymmetrically broadened. The authors of Ref. 4 attributed the observed TO-type mode to the breaking of the spherical symmetry of the InP QDs. However, further studies[8] have shown that the shape of chemically grown NCs is normally very close to spherical. Then we can ask whether the ODP mechanism is significant in QDs and how does the resulting interplay of the LO and TO scattering intensities actually work out? In the present Rapid Communication we are addressing these questions by obtaining a general expression for the probability of RRS assisted by LO and TO phonons, which allows us to explain the observed "anomalous" spectra and the TO-type mode in III-V QDs. Also, a criterion (indicating when the ODP contribution is negligible) is analyzed and the predictions of the theory are tested with the experimental data for InP NCs.

II. EXCITON-PHONON INTERACTIONS

The first-order RRS amplitude is determined by[1]

$$\mathcal{M}=\sum_{\kappa,\kappa'}\frac{\langle 0|H^{+}_{eR}(\mathbf{e}_S)|\kappa'\rangle\langle\kappa'|H^{\mathrm{DP}}_{ex-ph}+H^{F}_{ex-ph}|\kappa\rangle\langle\kappa|H^{-}_{eR}(\mathbf{e}_I)|0\rangle}{(E_{\kappa'}-\hbar\Omega_S)(E_{\kappa}-\hbar\Omega_I)}, \tag{1}$$

where $\mathbf{e}_I$ and Ω_I ($\mathbf{e}_S$ and Ω_S) are the polarization and frequency of the incident (scattered) photon, respectively, κ (κ') enumerates the excitonic states with the energy E_κ ($E_{\kappa'}$), $|0\rangle$ stands for the excitonic vacuum, and $H^{\pm}_{ex-R}$ is the exciton-radiation interaction Hamiltonian for the photon absorption and emission. The Fröhlich (H^{F}_{ex-ph}) and ODP (H^{DP}_{ex-ph}) exciton-phonon Hamiltonians are given by

$$H^{F}_{ex-ph}=\frac{C_F}{\sqrt{R}}\sum_{\nu}[\phi_\nu(\mathbf{r}_h)-\phi_\nu(\mathbf{r}_e)] \tag{2}$$

and

 ©2008 The American Physical Society

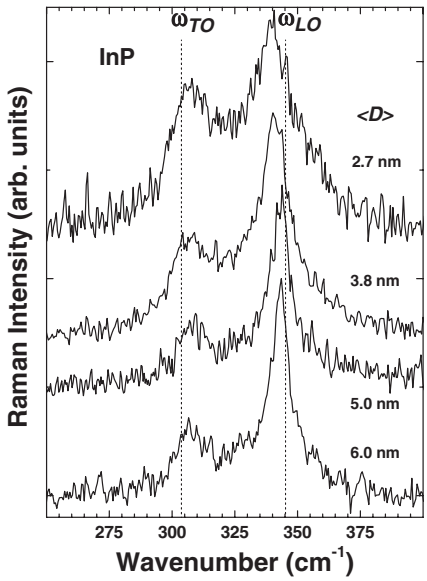

FIG. 1. Raman spectra of four matrix-free films of InP QDs with different mean diameter.

$$H_{ex-ph}^{\mathrm{DP}} = \frac{\sqrt{3}u_0 d_0}{2a_0} \sum_{\nu} [\mathbf{D}_e^{\nu} \cdot \mathbf{u}_{\nu}(\mathbf{r}_e) + \mathbf{D}_h^{\nu} \cdot \mathbf{u}_{\nu}(\mathbf{r}_h)], \qquad (3)$$

where $C_F = e\sqrt{2\pi\hbar\omega_{\mathrm{LO}}(\epsilon_\infty^{-1} - \epsilon_0^{-1})}$, ϵ_∞ and ϵ_0 are, respectively, the high-frequency and static dielectric constants of the QD material, R is the QD radius, $\phi_\nu(\mathbf{r})$ and $\mathbf{u}_\nu(\mathbf{r})$ are the dimensionless electrostatic potential and the relative displacement field, respectively, u_0 is the zero-phonon amplitude[1] (proportional to $R^{-3/2}$ due to the normalization condition), a_0 is the lattice constant, and $\mathbf{D}_p^{\nu}$ $(p=e,h)$ is the deformation potential (DP) vector as defined by Bir and Pikus.[9] In virtue of the symmetry, for a semiconductor with zinc-blend structure the conduction band does not contribute to the Raman tensor and d_0 corresponds to the ODP constant for the Γ_{15}^v band.[10]

Our theoretical description is based on the Luttinger-Kohn Hamiltonian.[11] Assuming infinite QD/matrix barriers and neglecting the electron-hole interaction, the excitonic states can be labeled by the electron-spin and hole momentum projections, $s_z = \pm 1/2$ and $M = \pm 1/2, \pm 3/2$.[12] Under resonance conditions with the lowest excitonic states, the main contribution to the scattering amplitude comes from the $1s_e - 1S_{3/2}$ octet. These states, with energy E_1, are all degenerate due to the above assumption.

We employ a continuum theory of optical phonons in order to calculate ϕ_ν and $\mathbf{u}_\nu$. Such an approach was developed from the earlier dielectric continuum (DC) model (see Ref. 13 for a review). In particular, the problem of $ex-ph$ interaction in a heterostructure was first treated using a modified DC model.[14] However, the phonons in this theory are dispersionless and therefore cannot reproduce the asymmetry of the observed Raman or far-infrared (FIR) line shape for II-VI QDs.[2,3] Incorporating the phonon dispersion, we obtain[15]

$$(\omega^2 - \omega_{\mathrm{TO}}^2)\mathbf{u} = \beta_L \nabla(\nabla \cdot \mathbf{u}) - \beta_T \nabla \times (\nabla \times \mathbf{u}) + \frac{\alpha}{\rho} \nabla \phi,$$

$$\nabla(\epsilon_\infty \nabla \phi - 4\pi\alpha\mathbf{u}) = 0,$$

where β_L (β_T) is the curvature parameter of the bulk LO (TO) phonon-dispersion curve, α is the polarizability per cation-anion pair, and ρ is the reduced atomic mass density.[16] Solving simultaneously the coupled elastic theory, equations of motion, and the Poisson equation allow fulfillment of the set of electrostatic and mechanical boundary conditions leading to the intermixing of confined LO, TO, and interface modes. This is a key issue for the correct description of the present experiments. The set of three "spherical" quantum numbers for the optical phonons is $\nu=\{l_p, m_p, n_p\}$ (l_p is the angular momentum, m_p is the z projection, and n_p is the radial quantum number). The expressions for $\phi_\nu(\mathbf{r})$ and $\mathbf{u}_\nu(\mathbf{r})$ are given elsewhere.[17–19]

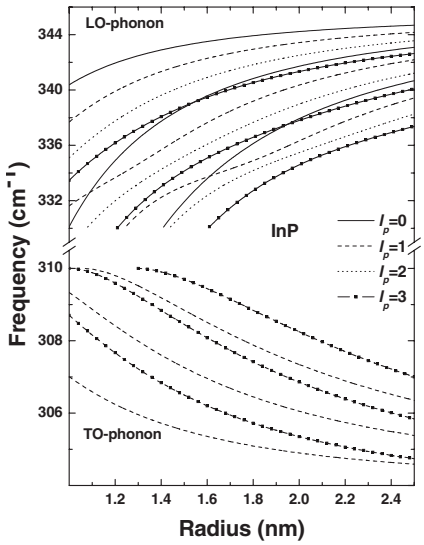

FIG. 2. Radial dependence of the optical phonon modes allowed to the first-order Raman scattering in InP QDs.

III. RAMAN SELECTION RULES

Fröhlich-type Hamiltonian leads (in the framework of the Luttinger-Kohn formalism) to the well-known Raman scattering selection rule for QD phonons with $l_p=0$ and $l_p=2$; $m_p=0, \pm 2$[3,20] (where the Z axis of the coordinate system for the phonon angular momentum is parallel to the photon wave vector). For the ODP interaction, we note that both the LO and TO phonons can produce interband transitions between the Γ_8-valence bands.[21] Since $\mathbf{u}_\nu \sim \nabla\phi_\nu$, the displacement vector presents an opposite parity with respect to $\phi_\nu(\mathbf{r})$ and the Raman tensor for deformation-potential Hamiltonian will be nonzero for phonons with $l_p=1$; $m_p=0$ and $l_p=3$; $m_p=0, \pm 2$. Figure 2 shows the dependence of the phonon frequencies ω_{l_p,n_p} (degenerate with respect to m_p) on the QD radius for the allowed LO $(l_p=0,1,2,3)$ and TO $(l_p=1,3)$ modes contributing to the Raman spectra. For the allowed excitonic transitions, we have $\Delta s_z=0$ and $\Delta M=0, \pm 2$.

IV. SCATTERING PROBABILITY

The total Raman cross section is proportional to the sum over all phonon modes ν of the scattering probabilities $W_\nu(\Omega_I, \Omega_S; e_I, e_S) = |\mathcal{M}_\nu|^2$. Since the ensemble of spherical QDs does not present any selected quantization axis, it is

necessary to average over all possible directions of the incident photon wave vector. Then it is convenient to work with the trace and the irreducible part of the Raman tensor responsible for so-called scalar and symmetric scattering,[22] respectively. Only diagonal $ex-ph$ matrix elements contribute to the trace (or scalar) term in a backscattering geometry. Thus, the scattering probability for $\mathbf{e}_S \| \mathbf{e}_I$ can be written as $W_\nu^{\mathbf{e}_S\|\mathbf{e}_I} = W_{\nu,\,\mathrm{sc}}^{\mathbf{e}_S\|\mathbf{e}_I} + W_{\nu,\,\mathrm{sy}}^{\mathbf{e}_S\|\mathbf{e}_I}$ with

$$W_{\nu,\,\mathrm{sc}}^{\mathbf{e}_S\|\mathbf{e}_I} = \frac{(2\pi)^3}{\Omega_I \Omega_S}\left(\sqrt{\frac{C_F}{3V}}\frac{ePK}{m_0 \eta R^{1/4}}\right)^4 [N(\omega_\nu)+1] \times \frac{\left|\sum_M \langle M|\phi_\nu + f\mathbf{D}_h^\nu \cdot \mathbf{u}_\nu|M\rangle - 4\langle s_z|\phi_\nu|s_z\rangle\right|^2}{(E_1-\hbar\Omega_I)^2(E_1-\hbar\Omega_S)^2} \times \delta(\Omega_I-\Omega_S-\omega_\nu), \quad (4)$$

where P is the Kane's momentum matrix element, K is the overlap integral of the electron and hole radial envelope functions,[12] m_0 (e) is the free-electron mass (charge), η is the refraction index of the medium, V is the volume, N denotes the Bose-Einstein function, and $f=\sqrt{3}Rd_0u_0/(2a_0C_F)\sim R^{-1}$ is a dimensionless parameter that measures the relative contribution of the Fröhlich and ODP mechanisms. The second independent term, due to the irreducible part of the Raman tensor, is determined by hole-phonon interaction and the corresponding scattering probability $W_{\nu,\,\mathrm{sy}}^{\mathbf{e}_S\|\mathbf{e}_I}$ is given by an expression similar to Eq. (4) but the numerator in the second line is replaced by $(|A|^2+|B|^2)/2$, where $A=\Sigma_M(-1)^{|M|-1/2}\langle M|\phi_\nu+f\mathbf{D}_h^\nu\cdot\mathbf{u}_\nu|M\rangle$, $B=\Sigma_M[\langle M|\phi_\nu+f\mathbf{D}_h^\nu\cdot\mathbf{u}_\nu|M'\rangle+\mathrm{C.C.}]$, the last sum over M is restricted to $-1/2$, $-3/2$, and $M'=M+2$. In the case of cross polarizations $(\mathbf{e}_S\perp\mathbf{e}_I)$, the contribution of the scalar part vanishes and the overall result equals to 3/4 of the corresponding value of the symmetric part for the $e_S\|e_I$ scattering amplitude, i.e., $W_\nu^{\mathbf{e}_S\perp\mathbf{e}_I}=\frac{3}{4}W_{\nu,\,\mathrm{sy}}^{\mathbf{e}_S\|\mathbf{e}_I}$.[3,22] Notice that according to the established selection rules, there is no interference effect between the two $ex-ph$ interactions.

V. EXPERIMENTAL DETAILS

We performed a RRS study of InP QDs produced by a colloidal chemistry technique[23] and deposited onto a glass substrate in the form of a matrix-free film. InP NCs were produced using essentially the same colloidal synthesis technology[8] as used for II-VI QDs. The dots were nearly spherical with the diameter ranging from 2.7 to 6.0 nm as determined by transmission electron microscopy studies. Polarized RRS spectra were measured at room temperature using a Jobin-Yvon T64000 spectrometer and an Ar^+ laser. Our experimental data are presented in Figs. 1, 3, and 4.

VI. COMPARISON BETWEEN THEORY AND EXPERIMENT

We evaluated W_ν in both scattering configurations $\bar{Z}(X,X)Z$ and $\bar{Z}(X,Y)Z$ for ensembles of InP QDs using the bulk phonon parameters.[24] The calculated scattering probability was averaged over a Gaussian distribution of the QD radius with a standard deviation of 10%. The results for two samples are shown in Figs. 3 and 4. The LO-type peak for $\mathbf{e}_S\|\mathbf{e}_I$ is formed mostly by the $l_p=0$ modes (see inset of Fig. 3) occupying only the frequency region approximately from 330 to 345 cm^{-1}. The quadrupolar $l_p=2$ modes appear in both polarizations giving the major contribution to the LO phonon part of the spectra for $\mathbf{e}_S\perp\mathbf{e}_I$. The deformation potential contributes substantially even for parallel polarization with $l_p=1$ and 3. It becomes clear that the anomalous TO-

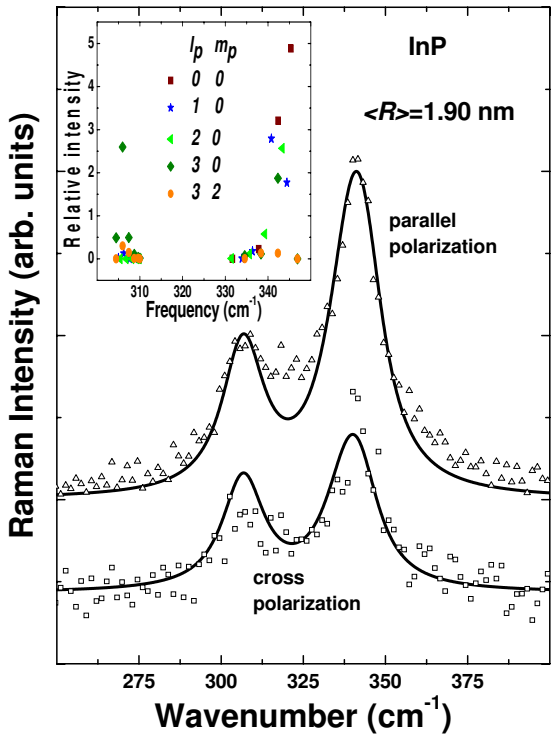

FIG. 3. (Color online) Experimental and calculated RRS spectra of InP QDs. The spectra were normalized to the peak value of the parallel polarization spectrum. Inset: The relative contributions of different phonon modes for $\mathbf{e}_S\|\mathbf{e}_I$.

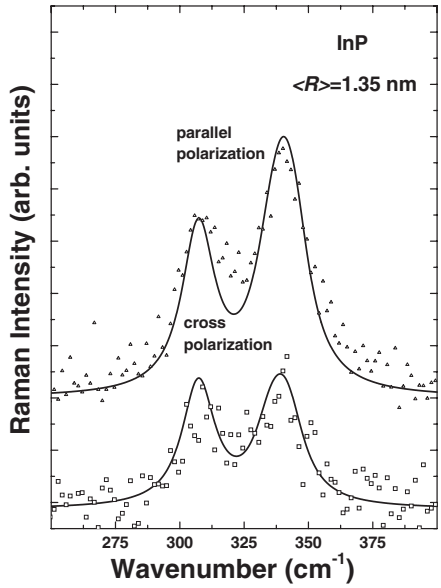

FIG. 4. Same as in Fig. 3 for $\langle R\rangle=1.35$ nm.

type peak is entirely due to the ODP interaction with the contribution of the $l_p=3$ modes dominating the spectra. From Figs. 3 and 4, we observe an increase in the relative intensity I_{TO}/I_{LO} as the QD mean radius decreases. This effect is clearly explained by the R dependence of the parameter f. For smaller radii, the relative contribution to the Raman cross section of the ODP with respect to the Fröhlich mechanism increases as R^{-2} [Eq. (4)]. Moreover, since $l_p=0$ modes do not contribute to the scattering in cross polarization, we expect that the I_{TO}/I_{LO} ratio should be higher for this configuration—in complete agreement with the experimental data. The dependence of the shift and broadening on $\langle R\rangle$ for both Raman peaks is explained by the radial dependence of ω_{l_p,n_p} (Fig. 2) originating from the bulk phonon bands, which are described by nearly parabolic dispersion curves with an upward and downward bending for the TO and LO branches, respectively.[25]

We have been able to fit quite well our experimental RRS spectra using solely the bulk values of the ODP constant and the parameters determining C_F. We have performed similar calculations for CdSe dots and found that the ODP interaction is negligible in the Raman spectra (f parameter is much smaller for CdSe than for InP). The importance of the ODP mechanism for III-V QDs is due to the lower ionic charge and larger d_0 characteristic of these materials compared to the II-VI ones. In fact, although less pronounced than for InP QDs, a TO-type mode has also been observed in Raman spectra of InAs dots.[3]

VII. CONCLUSION

The explanation of the presence of the TO-type mode in the Raman spectra of III-V QDs has been given in terms of the ODP mechanism that is enhanced because of the lower ionicity and higher d_0 values (compared to the II-VI materials) and due to its stronger dependence on R. Our study leads to two important conclusions. First, the short-range $ex-ph$ interaction, i.e., the ODP mechanism, becomes more important for QDs with small radii. It is responsible for the anomalous TO-type peak in the RRS spectra of spherical QDs. The calculations show that the Fröhlich matrix element scales as $R^{-1/2}$, while for ODP the characteristic scaling is $R^{-3/2}$. Second, the contribution of the $l_p=0$ modes to the LO-type peak is excluded for $\bar{Z}(X,Y)Z$ scattering by Raman selection rules and the relative intensity I_{TO}/I_{LO} increases. The excellent agreement between the theory and experiment, obtained by taking into consideration both the Fröhlich-type and ODP couplings and using only the standard deviation of the QD radius distribution as *ad hoc* parameter, demonstrates that the $ex-ph$ interaction mechanisms are the same in NCs as they are in bulk semiconductors. These interactions can be described by the same functional relations and characteristic parameters in QDs as small as 3 nm in diameter.

ACKNOWLEDGMENTS

This work was partially supported by the FCT (Portugal). The authors wish to thank A. Rogach and D. Talapin for their sample preparation and characterization.

*mikhail@fisica.uminho.pt

[1] M. Cardona, in *Light Scattering in Solids II*, Topics in Applied Physics Vol. 50, edited by M. Cardona and G. Güntherodt (Springer-Verlag, Heidelberg, 1982); C. Trallero-Giner, A. Cantarero, and M. Cardona, Phys. Rev. B **40**, 4030 (1989).

[2] C. Trallero-Giner, A. Debernardi, M. Cardona, E. Menendez-Proupin, and A. I. Ekimov, Phys. Rev. B **57**, 4664 (1998).

[3] A. G. Rolo and M. I. Vasilevskiy, J. Raman Spectrosc. **38**, 618 (2007).

[4] A. A. Guzelian *et al.*, J. Phys. Chem. **100**, 7212 (1996).

[5] M. J. Seong *et al.*, Appl. Phys. Lett. **82**, 185 (2003).

[6] F. S. Manciu *et al.*, Physica E (Amsterdam) **26**, 14 (2005).

[7] A. G. Rolo *et al.*, in *Proceedings of the 27th International Conference on the Physics of Semiconductors (ICPS27)*, AIP Conf. Proc. Vol. 772, edited by J. Menendez and C. G. Van de Walle (AIP, Melville, NY, 2005), pp. 675–676.

[8] A. L. Rogach, D. V. Talapin, and H. Weller, in *Colloids and Colloid Assemblies*, edited by F. Caruso (Wiley, Weinheim, 2004), pp. 52–95.

[9] G. L. Bir and G. E. Pikus, *Symmetry and Strain-Induced Effects in Semiconductors* (Wiley, New York, 1974).

[10] A. Blacha, H. Presing, and M. Cardona, Phys. Status Solidi B **126**, 11 (1984).

[11] J. M. Luttinger and W. Kohn, Phys. Rev. **97**, 869 (1955).

[12] A. L. Efros, M. Rosen, M. Kuno, M. Nirmal, D. J. Norris, and M. Bawendi, Phys. Rev. B **54**, 4843 (1996).

[13] M. A. Stroscio and M. Dutta, *Phonons in Nanostructures* (Cambridge University Press, Cambridge, England, 2001).

[14] L. Wendler, Phys. Status Solidi B **129**, 513 (1985).

[15] C. Trallero-Giner, R. Pérez-Alvarez, and F. García-Moliner, *Long Wave Polar Modes in Semiconductor Heterostructures* (Pergamon, London, 1998).

[16] Note that the limit $\beta_{L,T}\rightarrow 0$ corresponds to the model (Ref. 14).

[17] The functions ϕ_ν and u_ν are quite cumbersome and for simplicity are not written here. The calculation of exciton-phonon matrix elements are straightforward but somewhat tedious. Explicit mathematical form of the u_ν, ϕ_ν, and ω_ν for phonons in spherical QDs are given in Refs. 3, 18, and 19.

[18] E. Roca, C. Trallero-Giner, and M. Cardona, Phys. Rev. B **49**, 13704 (1994).

[19] M. I. Vasilevskiy, Phys. Rev. B **66**, 195326 (2002).

[20] E. Duval, Phys. Rev. B **46**, 5795 (1992).

[21] A. Dargys, Semicond. Sci. Technol. **20**, 733 (2005).

[22] V. B. Berestetskii, E. M. Lifshitz, and L. P. Pitaevskii, *Quantum Electrodynamics* (Pergamon, Oxford, 1982).

[23] D. V. Talapin *et al.*, J. Phys. Chem. B **106**, 12659 (2002).

[24] D. J. Lockwood, G. Yu, and N. L. Rowell, Solid State Commun. **136**, 404 (2005).

[25] To the best of our knowledge, TO phonon dispersion curves have not been measured experimentally while earlier calculations [P. H. Borcherds *et al.*, J. Phys. C **8**, 2022 (1975)] predicted that they are nearly flat. However, the asymmetry of the TO-type Raman peak and its blue shift for smaller QDs clearly indicate that bulk TO phonons with nonzero wave vector must have higher frequencies than the Γ-point ones, as it has been assumed in our calculations.